Published in final edited form as:
Cell Mol Bioeng. 2012 December ; 5(4): 488–492. doi:10.1007/s12195-012-0249-4.

Development of a Label-free Imaging Technique for the Quantification of Thrombus Formation

Sandra M. Baker, **Kevin G. Phillips**, and **Owen J. T. McCarty**
Department of Biomedical Engineering, School of Medicine, Oregon Health & Science University, 3303 SW Bond Ave, Portland, OR 97239, USA

Abstract

The characterization of platelet aggregation and thrombus formation typically requires the use of fluorescent labels followed by fluorescent confocal microscopy. However, fluorescent labels have been suspected to affect platelet function. We have developed a label-free imaging technique to characterize the volume and surface area coverage of platelet aggregates and thrombi formed under shear. Platelet aggregates were formed by perfusing anti-coagulated whole blood over fibrillar collagen. Thrombi were formed by perfusing recalcified whole blood over fibrillar collagen in the presence of coagulation. Platelet aggregates and thrombi volume and surface area coverage were quantified using a Hilbert transform differential interference contrast (DIC) microscopy technique (HT-DIC). Our data indicate that platelet aggregates and thrombi formed at a shear rate of 200 s^{-1} had similar volume and surface area coverage. At a shear rate of 1000 s^{-1}, both the volume and surface area coverage of platelet aggregates significantly increased as compared to low shear conditions. In contrast, the volume of thrombi formed in the presence of coagulation appeared to remain the same at both low and high shear rates. Utilization of this HT-DIC imaging technique can allow for insights into the kinetics and mechanisms by which thrombi are formed under various shear conditions in a label-free manner.

Keywords

Coagulation; Blood; Microscopy

Differential interference contrast microscopy is now a ubiquitous imaging modality due to its unique phase contrast enhancement ability. DIC image contrast is produced by phase gradients in transmitted waves through weak index contrast specimens, enabling high definition imaging of unstained samples that otherwise would appear semi-transparent using traditional bright field microscopy techniques.[1,7] Phase gradients in the transmitted field through the sample arise from either height changes, mass density variations, or the product of the two along the optical path taken by waves through the sample.[8–10] DIC images are not amenable to thresh-holding due to the overlap of gray level intensities of the imaged specimen with the background substrate upon which the sample is mounted. This failure to isolate details of the sample from the background makes additional processing of the image necessary in order to extract quantitative information.[1]

Address correspondence to Owen J. T. McCarty, Department of Biomedical Engineering, School of Medicine, Oregon Health & Science University, 3303 SW Bond Ave, Portland, OR 97239, USA. mccartyo@ohsu.edu.

Conflict of Interest: None.

Associate Editor Daniel Fletcher oversaw the review of this article.

The Hilbert transform is a spatial frequency space multiplier operator that creates symmetric image features through the maintenance of positive frequency components and the reversal of negative frequency components.[1,12] The utility of the transform lays in its ability to remove the *bas relief* of DIC images, thus enabling the ability to threshold the background intensity values out of the image (Fig. 1a). The application of a Hilbert transform to DIC images, referred to as HT-DIC, is a simple non-iterative fast-Fourier transform based image processing method that can quickly be applied to the imagery of biological specimens.

The ability to threshold the image comes with the artificial introduction of low frequency noise components which give rise to axial blurring (Fig. 1a, top right). We introduce the application of a high-pass Fourier filter to eliminate this axial blurring to facilitate edge detection of specimens in DIC image cubes (Fig. 1a, bottom right). Using this high-pass filtered HT-DIC post processing procedure we investigated the geometric parameters of platelet aggregates and thrombi formed under conditions of shear.

Through-focus DIC imaging of samples were performed at ×40 magnification with an oil-coupled, NA of 1.4 objective lens on a Zeiss Axio Imager 2 microscope (Carl Zeiss MicroImaging GmbH, Germany). 300 through-focus transverse DIC images with an illumination condenser NA of 0.9 were separated by a 0.1 μm axial increment. The microscope was operated under the control of SlideBook 5.5 (Intelligent Imaging Innovations, Denver, CO). To obtain volume measurements, the cross-sectional planes of the HT-DIC images of the sample were detected using a Sobel-based edge detection with the area computed in each plane and then added together using a custom program written in MATLAB® (The MathWorks, Inc., USA). Area measurements were determined by outlining *en face* HT-DIC images at the central focal position of the image cube.

To validate the HT-DIC method, average surface area coverage and volume of ten 7.67 ± 0.38 μm diameter fluorescein polystyrene microspheres (Bangs Laboratory, Inc., Fishers, IN) were measured using both confocal fluorescence microscopy and our HT-DIC technique (Figs. 1c, 1d). Confocal fluorescent microscopy was performed on a Zeiss Elyra PS.1/LSM 710 microscope (Carl Zeiss MicroImaging GmbH, Germany) and microspheres were imaged and analyzed using the Zen 2011 imaging software (Carl Zeiss MicroImaging GmbH, Germany). The confocal fluorescence microscopy software calculated mean surface area coverage to be 50.3 ± 5.3 μm^2 and mean volume to be 228.0 ± 40.7 μm^3 for the 10 microspheres. The HT-DIC technique calculated mean surface area coverage to be 46.6 ± 2.9 μm^2 and mean volume to be 243.3 ± 21.5 μm^3 for the microspheres. According to the manufacturer specifications, actual surface area coverage and volume of the fluorescein microspheres was 46.2 ± 4.6 μm^2 and 236.3 ± 35.5 μm^3. This validation demonstrates that the HT-DIC technique is equivalent to confocal fluorescence microscopy in estimating geometric sample parameters.

To investigate the range of validity of the HT-DIC method to measure volume, 10 different (0.95 ± 0.10 μm, 4.82 ± 0.59 μm, 9.86 ± 0.65 μm, and 20.92 ± 0.64 μm diameter (Bangs Laboratory, Inc., Fishers, IN)) polystyrene microspheres were analyzed. The actual manufacturer surface area coverage and volume of the microspheres were compared to values calculated using our HT-DIC technique (Figs. 1e, 1f). The HT-DIC technique was determined to be within the manufacturing variation of the microspheres in the range of 1–20 μm diameter samples. As expected, the HT-DIC method failed for 0.1 micron polystyrene microspheres (data not shown), as they are below the diffraction limit of optical microscopy (~0.25 μm).[6]

Having validated the HT-DIC method we applied the technique to characterize surface area coverage and volume measurement of platelet aggregates and thrombi under two different

physiological shear rates.[11] With the purpose of generating platelet aggregates under flow (Figs. 1b, 2a), venous blood was collected from healthy volunteers into D-phenylalanyl-L-prolyl-L-arginine chloromethyl ketone (PPACK, 40 μmol/L).[14] Whole blood collected into PPACK was supplemented with 10 μmol/L PPACK every hour to maintain inactivation of coagulation factors, resulting in only platelet-collagen adhesion and platelet–platelet aggregations. Glass capillary vitrotubes (0.2 × 2.0 × 50 mm, Vitrotube™ Catalog #5002, VitroCom, Mountain Lakes, NJ) were coated with fibrillar collagen (100 μg/mL, 1 h at 25 °C) followed by washing with PBS and blocking with BSA (5 mg/mL, 1 h at 25°C).[12] Collagen-coated vitrotubes were assembled onto microscope slides and mounted onto the stage of an inverted microscope (Zeiss Axiovert 200 M, Carl Zeiss MicroImaging GmbH, Germany).[3] A pulse-free syringe pump perfused PPACK-anticoagulated blood through the flow chamber for 5 min to form platelet aggregates on the collagen surface at physiologically relevant shear rates of either 200 s^{-1} or 1000 s^{-1}.[4,5]

In order to form thrombi under shear in the presence of coagulation, venous blood was collected from healthy volunteers into one-tenth sodium citrate (NaCit, 0.38% w/v). To trigger coagulation and drive fibrin formation, a separate syringe pump mixed calcium flow buffer (75 mmol/L $CaCl_2$ and 37.5 mmol/L $MgCl_2$) with the sodium citrate-anticoagulated blood immediately prior to perfusion through the flow chamber.[4,13,14] A representative image of thrombus formed under shear is shown in Fig. 2b.

Vitrotubes containing either platelet aggregates or thrombi were washed for 5 min with modified Hepes/Tyrode buffer (136 mmol/L NaCl, 2.7 mmol/L KCl, 10 mmol/L Hepes, 2 mmol/L $MgCl_2$, 2 mmol/L $CaCl_2$, 5.6 mmol/L glucose, 0.1% BSA; pH 7.45) at the same shear rate to remove unbound blood components. The samples were fixed with paraformaldehyde (PFA, 4%) for image analysis.[2,3]

Experiments were repeated using blood from three different donors. *Z*-stack images from three random fields of view (215 μm × 160 μm*)* were processed for each sample, resulting in a total of nine *z*-stack images for each treatment. *Z*-stack images were taken from the surface of the slide to 5 μm above the platelet aggregates or thrombi.

Figures 2c, 2d, 2e, and 2f show the histograms of surface area coverage and volume of individual platelet aggregates and thrombi formed at 200 s^{-1} and 1000 s^{-1} shear rates. Table 1 displays the range for the greatest frequency (peak) for surface area coverage and volume of individual platelet aggregates and thrombi. Figures 2c and 2d display mean total surface area coverage of platelet aggregates and thrombi formed at 200 s^{-1} and 1000 s^{-1} for a 215 μm by 160 μm field of view, while Figs. 2e and 2f show mean total volume of platelet aggregates and thrombi for the field of view formed at 200 s^{-1} and 1000 s^{-1}.

We demonstrate the utility of a Hilbert transform differential interference contrast microscopy technique to quantify platelet aggregate and thrombi surface area coverage and volume.

Our data indicates that the surface area coverage and volume of platelet aggregates increases with shear. Platelet aggregate mean total surface area coverage for the 215 μm by 160 μm field of view increased from 10,091 ± 531 μm^2 at 200 s^{-1} to 18,393 ± 2040 μm^2 at 1000 s^{-1}, with a p value of 0.017. Platelet aggregate mean total volume for the field of view increased from 15,948 ± 2146 μm^3 at 200 s^{-1} to 42,937 ± 10,672 μm^3 at 1000 s^{-1}, with a p value of 0.036. However, under conditions of coagulation, the surface area coverage of thrombi increases with shear while the volume appears to remain constant. Thrombi mean total surface area coverage for the same size field of view increased from 8982 ± 1567 μm^2 at 200 s^{-1} to 14,527 ± 909 μm^2 at 1000 s^{-1}, with a p value of 0.038. Thrombi mean total volume for the field of view increased from 29,761 ± 7235 μm^3 at 200 s^{-1} to 34,349 ± 5991

μm^3 at 1000 s^{-1}, with a p value of 0.651. Utilization of this HT-DIC imaging technique can allow for insights into the kinetics and mechanisms by which thrombi are formed under various shear conditions in a label-free manner.

Acknowledgments

The authors would like to thank the reviewers for their constructive and useful criticisms of the original draft. The authors would also like to thank Stefanie Kaech Petrie of the Advanced Light Microscopy Core at The Jungers Center for use of their confocal microscope and Kathleen Rees for her work in image processing. This research was supported by the NIH grant R01HL101972.

References

1. Arnison MR, Cogswell CJ, Smith NI, Fekete PW, Larkin KG. Using the Hilbert transform for 3D visualization of differential interference contrast microscope images. J Microsc. 2000; 199:79–84.
2. Aslan JE, Itakura A, Gertz JM, McCarty OJ. Platelet shape change and spreading. Methods Mol Biol. 2012; 788:91–100. [PubMed: 22130702]
3. Aslan JE, Tormoen GW, Loren CP, Pang J, McCarty OJ. S6K1 and mTOR regulate Rac1-driven platelet activation and aggregation. Blood. 2011; 118:3129–3136. [PubMed: 21757621]
4. Berny MA, Munnix IC, Auger JM, Schols SE, Cosemans JM, Panizzi P, Bock PE, Watson SP, McCarty OJ, Heemskerk JW. Spatial distribution of factor Xa, thrombin, and fibrin(ogen) on thrombi at venous shear. PLoS ONE. 2010; 5:e10415. [PubMed: 20454680]
5. De Clerck L, Bridts C, Mertens A, Moens M, Stevens W. Use of fluorescent dyes in the determination of adherence of human leucocytes to endothelial cells and the effect of fluorochromes on cellular function. J Immunol Methods. 1994; 172:115–124. [PubMed: 8207260]
6. De Lange F, Cambi A, Huijbens R, de Bakker B, Rensen W, Garcia-Parajo M, van Hulst N, Figdor C. Cell biology beyond the diffraction limit: near-field scanning optical microscopy. J Cell Sci. 2001; 114:4153–4160. [PubMed: 11739648]
7. Lee S, Roichman Y, Yi G, Kim S, Yang S, van Blaaderen A, van Oostrum P, Grier DG. Characterizing and tracking single colloidal particles with video holographic microscopy. Opt Express. 2007; 15:18275–18282. [PubMed: 19551125]
8. Phillips K, Kolatkar A, Rees K, Rigg R, Marrinucci D, Luttgen M, Bethel K, Kuhn P, McCarty O. Quantification of cellular volume and sub-cellular density fluctuations: comparison of normal peripheral blood cells and circulating tumor cells identified in a breast cancer patient. Front Oncol. 2012; 2:96.
9. Preza, C.; King, S.; Dragomir, N.; Cogswell, C. Handbook of Biomedical Optics. Boas, D.; Pitris, C.; Ramanujam, N., editors. Charlestown: Taylor and Francis Books; 2011.
10. Preza C, Munster E, Aten J, Snyder D, Rosenberger F. Determination of direction-independent optical path-length distribution of cells using rotational-diversity transmitted-light differential interference contrast (DIC) images. Image Acquis Process. 1998; 3261:60–70.
11. Tangelder G, Slaap D, Arts T, Reneman R. Wall shear rate in arterioles in vivo: least estimates from platelet velocity profiles. Am J Physiol. 1988; 254:H1059–H1064. [PubMed: 3381893]
12. van Munster E, van Vliet L, Aten J. Reconstruction of optical pathlength distributions from images obtained by a wide-field differential interference contrast microscope. J Microsc. 1997; 188:149–157. [PubMed: 9418272]
13. White TC, Berny MA, Robinson DK, Yin H, DeGrado WF, Hanson SR, McCarty OJ. The leech product saratin is a potent inhibitor of platelet integrin alpha2beta1 and von Willebrand factor binding to collagen. FEBS J. 2007; 274:1481–1491. [PubMed: 17489103]
14. White-Adams TC, Berny MA, Patel IA, Tucker EI, Gailani D, Gruber A, McCarty OJ. Laminin promotes coagulation and thrombus formation in a factor XII-dependent manner. J Thromb Haemost. 2010; 8:1295–1301. [PubMed: 20796202]

Abbreviations

BSA	Bovine serum albumin
DIC	Differential interference contrast
NA	Numerical aperture
PBS	Phosphate buffered saline

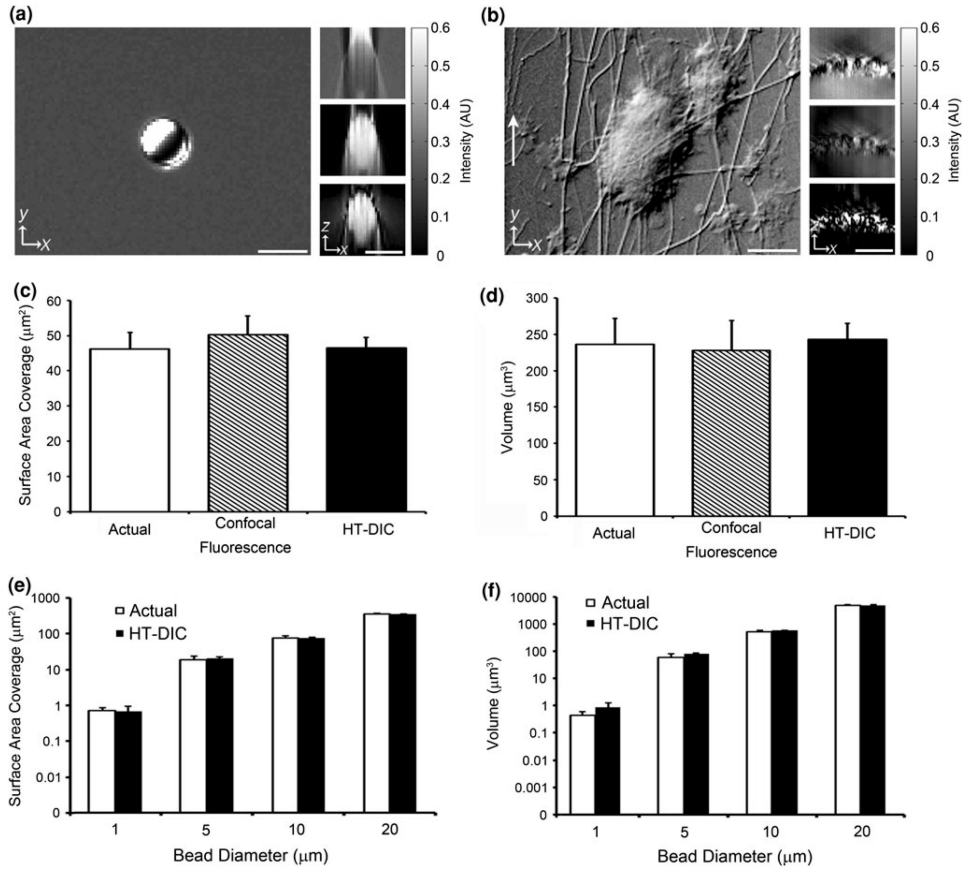

Figure 1.

Validation of HT-DIC imaging technique. (a) Sagittal ×40 DIC image of a 4.82 ± 0.59 μm diameter polystyrene microsphere bead (left). Cross-sectional view of the DIC *z*-stack images (top right), Hilbert transformed DIC *z*-stack (middle right), and high-pass filtered Hilbert transformed DIC *z*-stack (bottom right) of the microsphere. (b) Sagittal DIC image of a platelet aggregate formed at 200 s^{-1} shear rate (left). Cross-sectional view of the DIC *z*-stack images (top right), Hilbert transformed DIC *z*-stack (middle right), and high-pass filtered Hilbert transformed DIC *z*-stack (bottom right) of the platelet aggregate. The direction of flow is indicated by the white arrow. Intensity values are in arbitrary units. Scale bars represent 5 μm. (c and d)Mean surface area coverage and volume of ten 7.67 ± 0.38 μm diameter fluorescein polystyrene microspheres calculated using confocal fluorescence microscopy and the HT-DIC technique. The actual surface area coverage and volume of the spheres using the manufacturer specifications are also plotted. Error bars are ± standard deviation. (e and f) Mean surface area coverage and volume for ten 0.95 ± 0.10 μm, 4.82 ± 0.59 μm, 9.86 ± 0.65 μm, and 20.92 ± 0.64 μm diameter uniform polystyrene microspheres calculated using the HT-DIC technique. Results are plotted against the actual values for the spheres according to the manufacturer. Error bars are ± standard deviation.

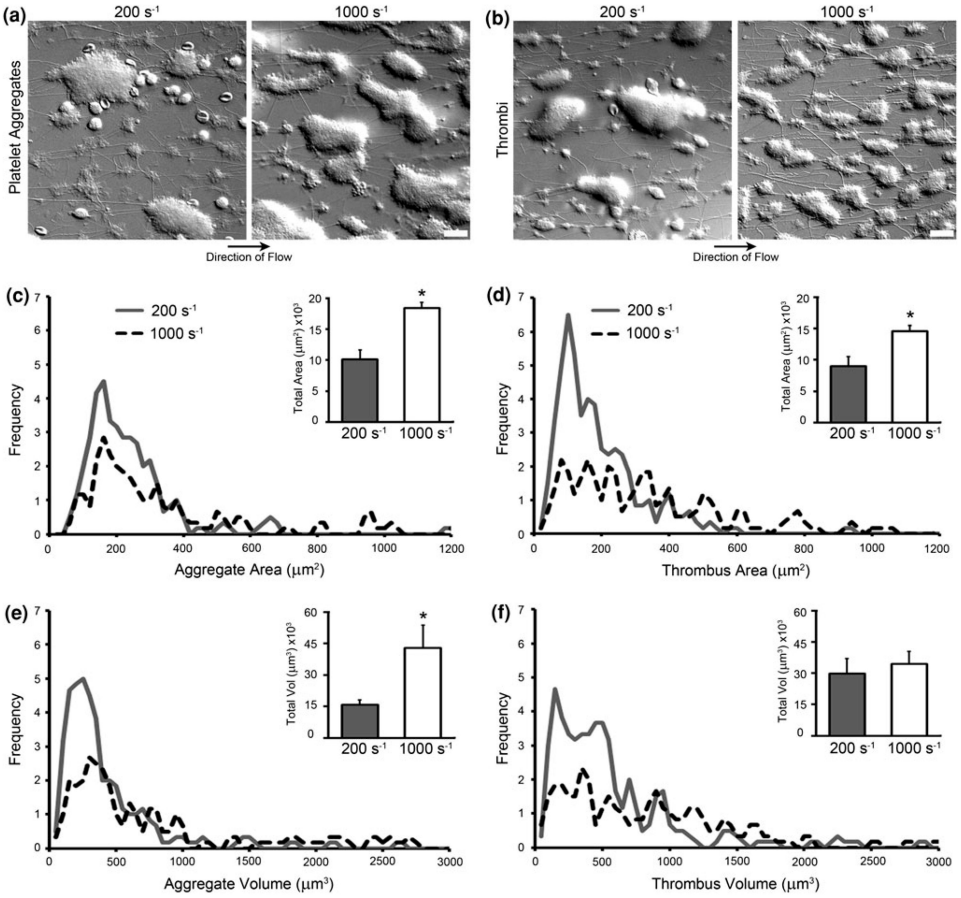

Figure 2.

Platelet aggregate and thrombi surface area coverage and volume. (a) DIC image of platelet aggregates formed at 200 s^{-1} and 1000 s^{-1} shear rates. (b) DIC images of thrombi formed at 200 s^{-1} and 1000 s^{-1} shear rates. All scale bars represent 20 μm. (c, d, e, and f) Histograms of aggregate and thrombus surface area coverage and volume for 200 s^{-1} and 1000 s^{-1} shear rates collected over three trials. The surface area coverage histograms used 20 μm^2 size bins, while the volume histograms used 50 μm^3 bins. Inlaid bar graphs display mean total aggregate and thrombus surface area coverage and volume for a 215 μm by 160 μm field of view. Error bars are ± SEM. Asterisks denote a p value ≤0.05 in comparison to 200 s^{-1} shear rate values.

Table 1

Range of greatest frequency for surface area coverage and volume of individual platelet aggregates and thrombi at 200 s^{-1} and 1000 s^{-1}.

	Platelet aggregates		Thrombi	
Shear rate	**Surface area coverage (μm^2)**	**Volume (μm^3)**	**Surface area coverage (μm^2)**	**Volume (μm^3)**
200 s^{-1}	140–180	150–250	80–120	50–150
1000 s^{-1}	140–160	300–400	60–100	300–400